Supporting Information

Isomeric spiro-[acridine-9,9'-fluorene]-2,4-dipyridylpyrimidine based TADF emitters: Insights into photophysical behaviors and OLED performances.

Paramaguru Ganesan,[‡,a] Deng-Gao Chen,[‡,b] Jia-Ling Liao,[a] Wei-Cheng Li,[c] Yi-Ning Lai,[c] Dian Luo,[c] Chih-Hao Chang,*[,c] Chang-Lun Ko,[d] Wen-Yi Hung,*[,d] Shun-Wei Liu,[e] Gene-Hsiang Lee,[b] Pi-Tai Chou,*[,b] and Yun Chi*[,a,f]

[a] Department of Chemistry, National Tsing Hua University, Hsinchu 30013, Taiwan

[b] Department of Chemistry, National Taiwan University, Taipei 10617, Taiwan

[c] Department of Photonics Engineering, Yuan Ze University, Chung-Li 32003, Taiwan

[d] Institute of Optoelectronic Sciences, National Taiwan Ocean University, Keelung 202, Taiwan

[e] Department of Electronic Engineering, Ming Chi University of Technology, New Taipei 24301, Taiwan

[f] Department of Materials Science and Engineering and Department of Chemistry, City University of Hong Kong, Hong Kong SAR

Table of Contents

Experimental Section

General Procedures. Solvents were dried over appropriate drying agents and commercially available reagents were used without further purification. All reactions were conducted under nitrogen atmosphere unless otherwise noted. 10H-Spiro[acridine-9,9-fluorene] was obtained from a multistep protocol starting from 2-bromo-N-phenylaniline, which was synthesized from coupling of 1-bromo-2-iodobenzene and aniline in the presence of $[Pd(dppf)_2Cl_2]$. After being lithiated with n-BuLi in hexane (2.5 M), it was coupled with 9-fluorenone and then cyclized in the presence of methanesulfonic acid.[1] Picolinimidamide hydrochloride, nicotinimidamide hydrochloride and isonicotinimidamide hydrochloride was synthesised from the literature method.[2] Parent chalcone (**1**) was synthesized according to our previous method,[3] while other derivatives **2** ~ **4** were prepared using pyridyl substituted starting material under analogous procedures.

All reactions were monitored by pre-coated TLC plates (0.20 mm with fluorescent indicator F_{254}). Mass spectra were obtained on a JEOL SX-102A instrument operating in electron impact (EI) or fast atom bombardment (FAB) mode. The ^1H, and ^{13}C NMR spectra were recorded on a Varian Mercury-400 or an INOVA-500 instrument. Elemental analysis was carried out with a Heraeus CHN-O-Rapid Elemental Analyzer. Thermal analysis was performed using a Seiko Instrument TG/DTA 320 thermogravimetric analyzer at a heating rate of 10 °C/min and under nitrogen. Differential scanning calorimeter (DSC) was conducted using a Seiko Instrument DSC220C, with a heating and cooling rate of 10 °C /min.

Synthesis of chalcone (**2**): To a stirring solution of 4-bromobenzaldehyde (5.0 g, 27.0 mmol), and Na_2CO_3 (5.73 g, 54 mmol) in water (60 mL)/methanol (30 mL) medium, 2-acetyl pyridine (3.27 g, 27 mmol) was added dropwise and then the solution was stirred at RT for overnight. During the course of the reaction, solid materials were precipitated from the reaction mixture. The solid was filtered, washed with cold ethanol and water, and recrystallized from ethanol to yield a white solid (**2**, 2.5 g, 58 %). The functionalized chalcone derivatives (**3** and **4**) were prepared analogously.

Characterization of **2**: ^1H NMR (400 MHz, $CDCl_3$, 298 K): δ 8.74 (d, *J* = 4.0 Hz, 1H), 8.29 (d,

J = 16.1 Hz, 1H), 8.19 (d, *J* = 7.9 Hz, 1H), 7.91 – 7.82 (m, 2H), 7.61 – 7.53 (m, 4H), 7.52 – 7.47 (m, 1H). MS(EI), *m/z* 287.1 $[M]^+$.

Characterization of **3**: ^{1}H NMR (400 MHz, acetone-d_6, 298 K): δ 9.30 (s, 1H), 8.80 (d, *J* = 4.8 Hz, 1H), 8.43 (d, *J* = 7.9 Hz, 1H), 7.93 (d, *J* = 15.7 Hz, 1H), 7.83 (d, *J* = 8.4 Hz, 2H), 7.79 (d, *J* = 15.7 Hz, 1H), 7.65 (d, *J* = 8.3 Hz, 2H), 7.56 (dd, *J* = 8.0, 4.8 Hz, 1H). MS(EI), *m/z* 287.1 $[M]^+$.

Characterization of **4**: ^{1}H NMR (400 MHz, DMSO-d_6, 298 K): δ 8.82 (d, *J* = 5.4 Hz, 2H), 7.97 (d, *J* = 5.4 Hz, 2H), 7.91 (d, *J* = 15.7 Hz, 1H), 7.85 (d, *J* = 8.4 Hz, 2H), 7.74 (d, *J* = 15.7 Hz, 1H), 7.66 (d, *J* = 8.4 Hz, 2H). MS(EI), *m/z* 287.0 $[M]^+$.

Synthesis of 4-(4-bromophenyl)-2,6-di(pyridin-2-yl)pyrimidine (**10**): A mixture of 3-(4-bromophenyl)-1-(pyridin-2-yl)prop-2-en-1-one (**2**, 2.74 g, 9.5 mmol) and picolinimidamide hydrochloride (**6**, 1.0 g, 6.3 mmol) in ethanol (40 mL) was heated to reflux. Potassium hydroxide (1.14 g, 20.3 mmol) in minimum amount of water (5 mL) was added dropwise to the refluxing mixture. After being stirred for overnight, during the course of the reaction solid materials were precipitated from the reaction mixture. The solid was filtered, washed with ethanol and water to yield a white solid (10, 1.5 g, 47 %). Other 4-bromopyridyl pyrimidine compounds (**11**) and (**12**) were prepared by coupling of chalcones **3** and **4** with corresponding imidamide salts **7** and **8** under identical condition.

Characterization of **10**: ^{1}H NMR (400 MHz, $CDCl_3$, 298 K): δ 8.89 (d, *J* = 4.8 Hz, 1H), 8.81 (s, 1H), 8.78 – 8.74 (m, 2H), 8.70 (d, *J* = 8.3 Hz, 1H), 8.26 (d, *J* = 8.0 Hz, 2H), 7.91 (t, *J* = 7.7 Hz, 2H), 7.67 (d, *J* = 8.0 Hz, 2H), 7.46 – 7.41 (m, 2H). MS(EI), *m/z* 388.1 $[M]^+$.

Characterization of **11**: ^{1}H NMR (400 MHz, DMSO, 298 K): δ 9.73 (s, 1H), 9.62 (s, 1H), 8.89 (d, *J* = 8.0 Hz, 1H), 8.82 (d, *J* = 7.9 Hz, 1H), 8.75 (dd, *J* = 10.5, 3.9 Hz, 2H), 8.70 (s, 1H), 8.46 (d, *J* = 7.0 Hz, 2H), 7.79 (d, *J* = 7.0 Hz, 2H), 7.60 (t, *J* = 11.4 Hz, 2H). MS(EI), *m/z* 387.9 $[M]^+$.

Characterization of **12**: ^{1}H NMR (400 MHz, DMSO, 298 K): δ 8.84 (d, *J* = 6.2 Hz, 4H), 8.81 (d, *J* = 7.1 Hz, 2H), 8.50 (d, *J* = 3.1 Hz, 2H), 8.48 (s, 1H), 8.43 (d, *J* = 5.8 Hz, 2H), 7.83 (d, *J* = 8.4 Hz, 2H). MS(EI), *m/z* 388.0 $[M]^+$.

Synthesis of 10-(4-(2,6-di(pyridin-2-yl)pyrimidin-4-yl)phenyl)-10H-spiro[acridine-9,9'-

fluorene] (**2NPMAF**): To a stirring solution of 4-(4-bromophenyl)-2,6-di(pyridin-2-yl)pyrimidine (**10**, 1.0 g, 2.57 mmol), 10H-spiro[acridine-9,9'-fluorene] (0.85 g, 2.57 mmol) and Bu^tONa (0.74 g, 7.71 mmol) in dry toluene (80 mL) at RT was added a solution of $Pd_2(dba)_3$ (0.24 g, 0.26 mmol) and $P(Bu^t)_3$ (0.10 g, 5.13 mmol) in dry toluene under N_2. The solution was refluxed for 48 hours and then cooled down to RT. The solution was concentrated to dryness and the residue was extracted with ethyl acetate (2 × 75 mL). This solution was washed with brine, dried over Na_2SO_4, and concentrated by rotary evaporation. The resulting residue was purified by silica gel column chromatography, eluting with hexane and ethyl acetate (1:1) to afford **2NPMAF** as pale yellow solid (0.74 g, 45 %). Other derivatives **PhPMAF, 3NPMAF** and **4NPMAF** were prepared under identical condition.

Characterization of **2NPMAF**: ^{1}H NMR (400 MHz, $CDCl_3$, 298 K): δ 8.99 (s, 1H), 8.96 (d, *J* = 4.5 Hz, 1H), 8.85 (d, *J* = 8.0 Hz, 1H), 8.82 – 8.77 (m, 2H), 8.70 (d, *J* = 8.1 Hz, 2H), 8.00 – 7.92 (m, 2H), 7.80 (d, *J* = 7.1 Hz, 2H), 7.70 (d, *J* = 8.0 Hz, 2H), 7.49 (dd, *J* = 8.4, 3.7 Hz, 2H), 7.45 (d, *J* = 7.5 Hz, 2H), 7.38 (t, *J* = 7.5 Hz, 2H), 7.28 (d, *J* = 7.5 Hz, 2H), 6.96 – 6.90 (m, 2H), 6.58 (t, *J* = 7.5 Hz, 2H), 6.45 – 6.40 (m, 4H). ^{13}C NMR (100 MHz, $CDCl_3$, 298 K): δ 165.13, 164.55, 163.91, 156.55, 155.32, 154.05, 150.18, 149.50, 143.63, 141.01, 139.19, 137.43, 137.19, 136.91, 131.82, 130.48, 128.37, 127.87, 127.56, 127.26, 125.70, 124.83, 124.15, 122.41, 120.74, 119.86, 114.60, 112.47, 56.78. MS(FAB), *m/z* 639.2 $[M]^+$. Anal. Calcd. for $C_{45}H_{29}N_5$: C, 84.48; H, 4.57; N, 10.95. Found: C, 84.53; H, 4.63; N, 10.69.

Characterization of **PhPMAF**: ^{1}H NMR (400 MHz, $CDCl_3$, 298 K): δ 8.78 (d, *J* = 8.0 Hz, 2H), 8.63 (d, *J* = 7.0 Hz, 2H), 8.36 (d, *J* = 6.4 Hz, 2H), 8.15 (s, 1H), 7.81 (d, *J* = 7.6 Hz, 2H), 7.71 (d, *J* = 7.0 Hz, 2H), 7.57 (dd, *J* = 16.3, 7.2 Hz, 6H), 7.46 (d, *J* = 7.5 Hz, 2H), 7.38 (t, *J* = 7.5 Hz, 2H), 7.27 (t, *J* = 7.7 Hz, 2H), 6.94 (t, *J* = 7.8 Hz, 2H), 6.59 (t, *J* = 7.5 Hz, 2H), 6.44 (t, *J* = 9.0 Hz, 4H). ^{13}C NMR (100 MHz, $CDCl_3$, 298 K): δ 165.09, 164.74, 163.93, 156.50, 143.51, 141.03, 139.21, 137.96, 137.74, 137.36 , 131.86, 130.97, 130.82, 130.08, 128.99, 128.53, 128.51, 128.37, 127.88, 127.60, 127.33, 127.26, 125.76, 124.90, 120.78, 119.90, 114.61, 110.50, 56.79. MS(FAB), *m/z* 637.3 $[M]^+$. Anal. Calcd. for $C_{47}H_{31}N_3$: C, 88.51; H, 4.90; N, 6.59. Found: C, 88.44; H, 4.89; N, 6.52.

Characterization of **3NPMAF**: ^{1}H NMR (400 MHz, $CDCl_3$, 298 K): δ 9.94 (s, 1H), 9.52 (s, 1H), 9.00 (d, *J* = 7.9 Hz, 1H), 8.82 (d, *J* = 4.9 Hz, 1H), 8.80 (d, *J* = 4.6 Hz, 1H), 8.66 (d, *J* = 8.1 Hz, 1H), 8.63 (d, *J* = 8.3 Hz, 2H), 8.22 (s, 1H), 7.80 (d, *J* = 6.9 Hz, 2H), 7.74 (d, *J* = 8.2 Hz, 2H), 7.55 (dd, *J* = 8.0, 4.9 Hz, 1H), 7.52 (dd, *J* = 8.0, 4.9 Hz, 1H), 7.44 (d, *J* = 7.6 Hz, 2H), 7.38 (t, *J* = 7.5 Hz, 2H), 7.28 (d, *J* = 7.5 Hz, 2H), 6.93 (t, *J* = 7.8 Hz, 2H), 6.59 (t, *J* = 7.5 Hz, 2H), 6.46 – 6.40 (m, 4H). ^{13}C NMR (100 MHz, $CDCl_3$, 298 K): δ 164.53, 163.38, 163.04, 156.44, 151.96, 151.71, 150.23, 148.64, 144.12, 140.94, 139.21, 136.83, 135.77, 134.79, 133.08, 132.64, 132.12, 130.13, 128.38, 127.93, 127.63, 127.27, 125.73, 124.97, 123.88, 123.45, 120.88, 119.92, 114.53, 111.05, 56.76. MS(FAB), *m/z* 639.2 $[M]^+$. Anal. Calcd. for $C_{45}H_{29}N_5$: C, 84.48; H, 4.57; N, 10.95. Found: C, 84.34; H, 4.48; N, 11.15.

Characterization of **4NPMAF**: ^{1}H NMR (400 MHz, $CDCl_3$, 298 K): δ 8.89 (dd, *J* = 9.2, 6.1 Hz, 4H), 8.63 (d, *J* = 8.3 Hz, 2H), 8.58 (d, *J* = 6.1 Hz, 2H), 8.28 (s, 1H), 8.19 (d, *J* = 6.2 Hz, 2H), 7.81 (d, *J* = 7.6 Hz, 2H), 7.75 (d, *J* = 8.3 Hz, 2H), 7.44 (d, *J* = 7.6 Hz, 2H), 7.38 (t, *J* = 7.5 Hz, 2H), 7.27 (t, *J* = 7.1 Hz, 2H), 6.94 (t, *J* = 7.8 Hz, 2H), 6.60 (t, *J* = 7.8 Hz, 2H), 6.47 – 6.39 (m, 4H). ^{13}C NMR (100 MHz, $CDCl_3$, 298 K): δ 165.09, 163.30, 163.18, 156.42, 150.95, 150.64, 144.65, 144.35, 144.00, 140.91, 139.22, 136.55, 132.22, 130.19, 128.38, 127.98, 127.65, 127.28, 125.71, 125.01, 122.23, 121.13, 120.93, 119.94, 114.49, 112.23, 56.75. MS(FAB), *m/z* 639.3 $[M]^+$. Anal. Calcd. for $C_{45}H_{29}N_5$: C, 84.48; H, 4.57; N, 10.95. Found: 84.47; H, 4.63; N, 10.88.

Photophysical Characterization: Steady-state absorption spectra were recorded using a Hitachi U-3310 spectrophotometer, and emission spectra were obtained using an Edinburgh FS920 fluorimeter. Time-resolved PL (PL decay curves) was measured by monitoring the decay of the intensity at the PL peak wavelength using the time-correlated single-photon counting (TCSPC) technique and nanosecond pulsed light excitation from a pulsed hydrogen-filled lamp (355 nm), with a fluorescence lifetime system (Edinburgh FLS920)

Single Crystal X-Ray Diffraction Studies. Single crystal X-ray diffraction data were measured on a Bruker SMART Apex CCD diffractometer using Mo radiation (λ = 0.71073 Å). The

data collection was executed using the *SMART* program. Cell refinement and data reduction were performed with the *SAINT* program. An empirical absorption was applied based on the symmetry-equivalent reflections and the *SADABS* program. The structures were solved using the *SHELXS-97* program and refined using *SHELXL-97* program by full-matrix least squares on F^2 values. CCDC-1855543 contains the supplementary crystallographic data of 3NPMAF. The data can be obtained free of charge from the Cambridge Crystallographic Data Centre via http://www.ccdc.cam.ac.uk.

OLED fabrication

Organic materials and the indium tin oxide (ITO)-coated glass with sheet resistance of ~15 Ω/square were purchased from Lumtec and Shine Materials Technology. The ITO substrate was washed with deionized water and acetone in sequence, followed by treatment with UV-Ozone for 5 minutes. All organic materials were subjected to temperature gradient sublimation. The organic and metal layers were deposited onto the ITO-coated glass substrate by thermal evaporation and the device fabrication was completed in a single cycle without breaking the vacuum. Shadow mask was used to define the active area (2 × 2 mm^2) of the device. Current density-voltage-luminance characterization was measured using two Keithley 2401 source meters equipped with a calibrated Si photodiode. The electroluminescent spectra were recorded using an Ocean Optics spectrometer.

Measurement and simulation of angle-dependent PL spectra

The experimental setup is composed of a half cylinder lens with a sample holder on a motorized rotation stage, a 10 kHz, 355-nm Nd:YAG Laser as continuous excitation source which is fixed behind of sample holder at an angle of 45°, a polarizer to select the p-polarization of the emitted light and a spectrometer (Ocean Optics USB2000+) to collect the PL spectra. The fluorescence is measured at different angles, from 0° to 90°, in steps of 2°. The measurements were repeated on different samples to ensure reproducible and consistent results. Analyzing the

angle-dependent PL of the film is performed using SETFOS 4.5 software in order to fit the ratio of horizontal dipoles (Θ) of the p-polarized light emission.

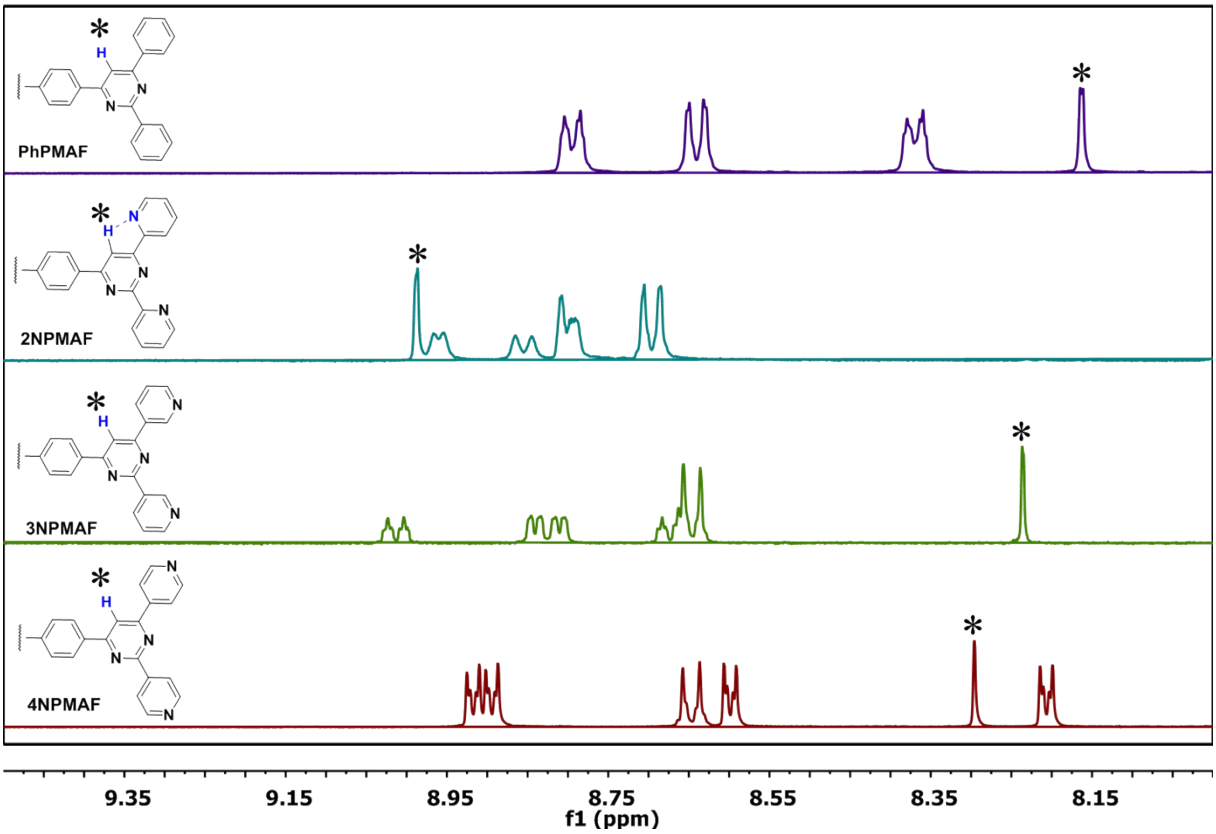

Figure S1. ^{1}H NMR spectra displaying the aromatic protons and signal of central pyrimidine unit. This pyrimidinyl proton is marked with asterisk in all derivatives, and the downfield shift of pyrimidinyl proton in **2NPMAF** is probably due to the intramolecular H-bonding interaction.

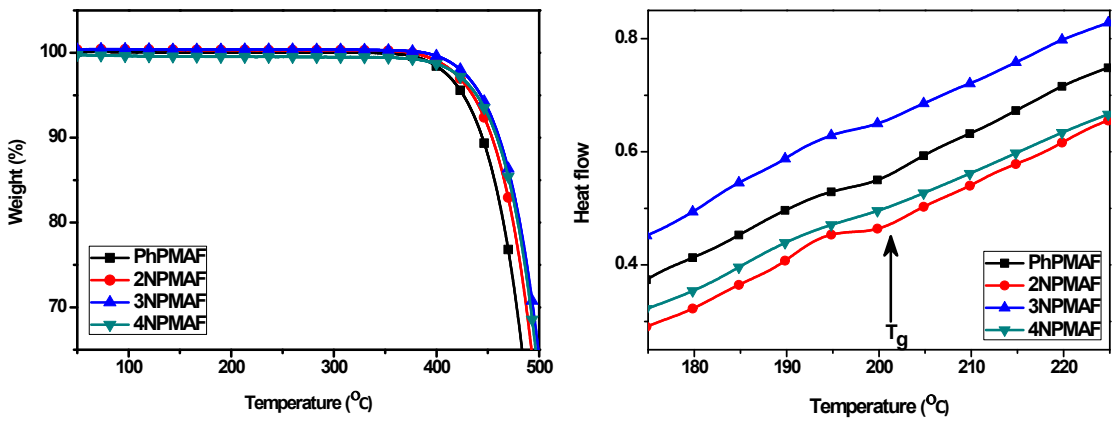

Figure S2. TGA (left) and DSC (right) data of **PhPMAF**, **2NPMAF**, **3NPMAF**, and **4NPMAF**. The samples were heated under a nitrogen atmosphere at a heating rate of 10 °C/min

Table S1. Thermal analysis of **PhPMAF**, **2NPMAF**, **3NPMAF**, and **4NPMAF**.[a]

	PhPMAF	**2NPMAF**	**3NPMAF**	**4NPMAF**
T_g (°C)	199	200	201	203
T_d (°C)[b]	426	435	443	439

[a] T_g, and T_d represent the glass transition, and decomposition temperatures respectively. [b] Temperature at 5% weight loss to initial weight.

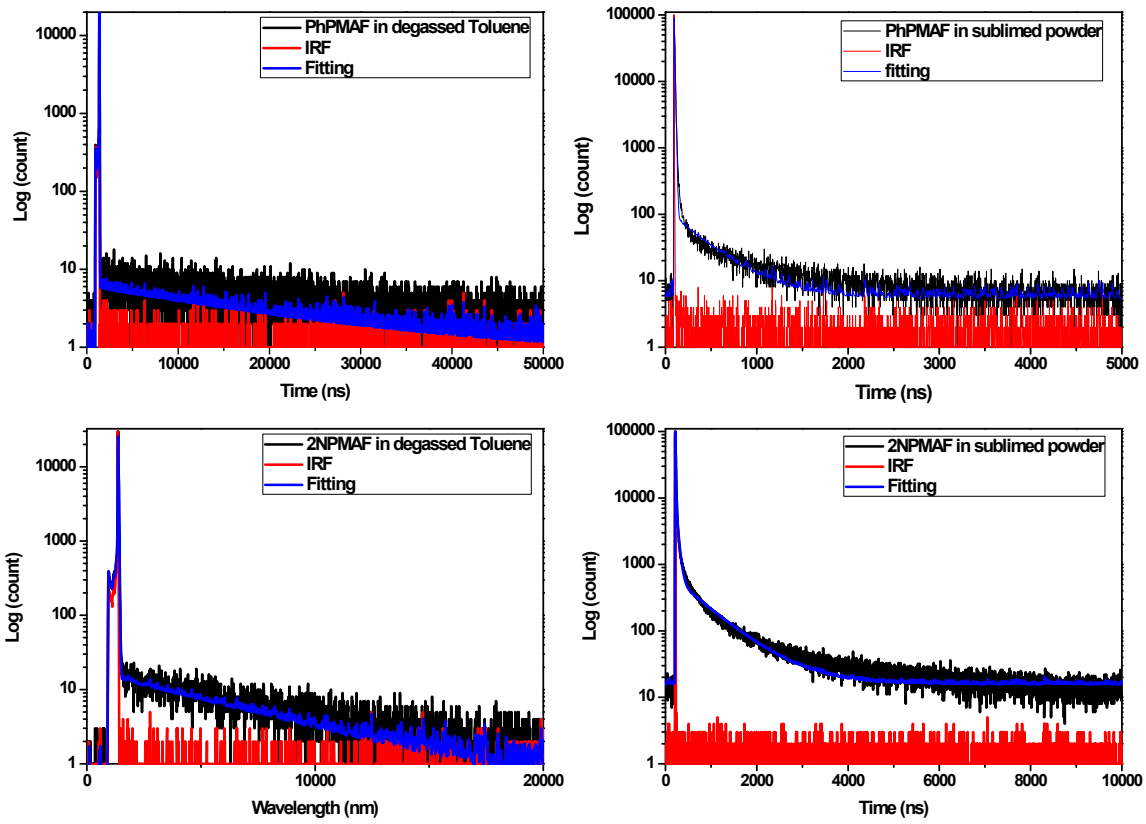

Figure S3. Transient photoluminescence characteristics of **PhPMAF** (top) and **2NPMAF** (bottom) in degassed toluene and sublimed powder (λ_{ex} = 374 nm). IRF=instrument response function (red).

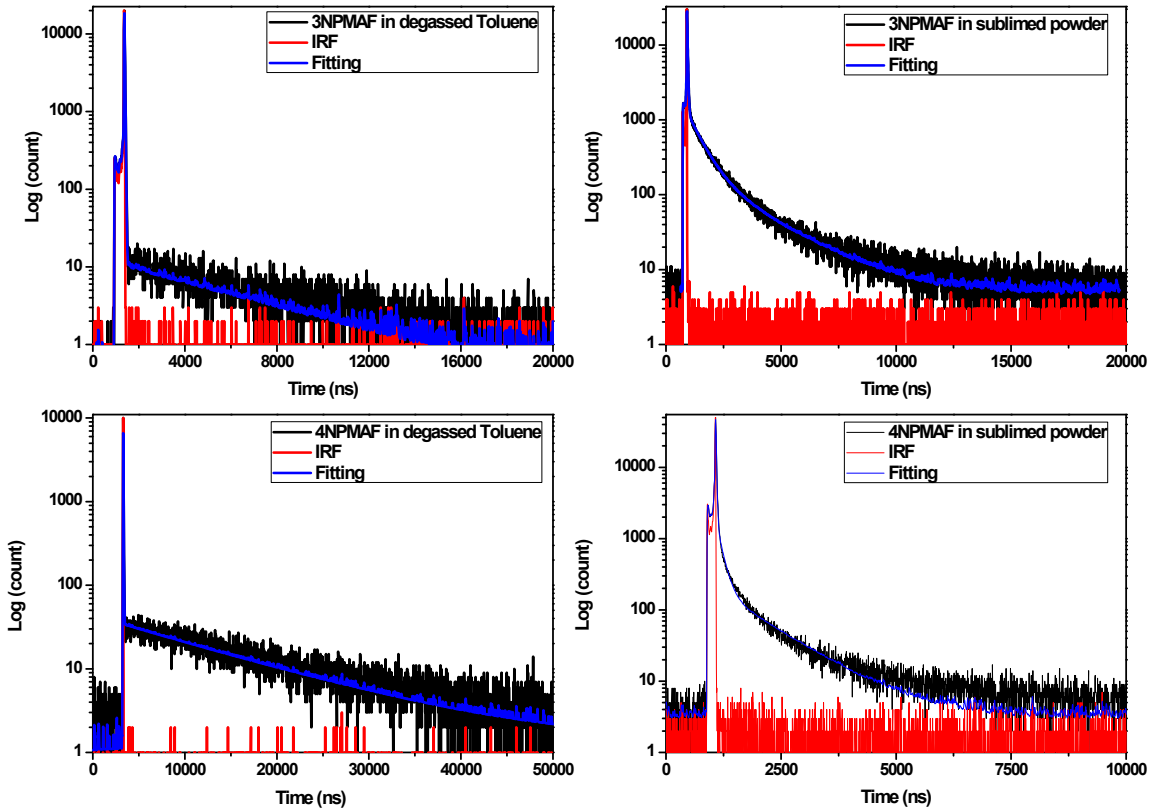

Figure S4. Transient photoluminescence characteristics of **3NPMAF** (top) and **4NPMAF** (bottom) in degassed toluene and sublimed powder (λ_{ex} = 374 nm). IRF=instrument response function (red).

Table S2. Photophysical properties of **PhPMAF**, **2NPMAF**, **3NPMAF** and **4NPMAF** under various states at RT and the calculated k_{isc} and k_{risc}.

	state	λ_{em} [nm]	$\tau_{1,2}$ [ns] and pre-exp. Factor $A_{1,2}$	k_{isc} (s^{-1})[a]	k_{risc} (s^{-1})[a]
PhPMAF	toluene	441	12 (0.9999), 10000 (0.0001)	8.33×10^7	8.33×10^3
	CH_2Cl_2	500	23 (0.9947), 3133 (0.0053)	4.32×10^7	2.30×10^5
	sublimed powder	447	6 (0.9991), 364 (0.0009)	1.67×10^8	1.50×10^5
	Co-doped DPEPO film	457	10 (0.9996), 1682 (0.0004)	9.99×10^7	4.00×10^4
2NPMAF	toluene	482	17 (0.9997), 5712 (0.0003)	5.88×10^7	1.76×10^4
	CH_2Cl_2	566	29 (0.9863), 1776 (0.0137)	3.24×10^7	2.09×10^6
	sublimed powder	477	8 (0.9363), 361 (0.0637)	1.17×10^8	7.96×10^6
	Co-doped DPEPO film	482	19 (0.9958), 1754 (0.0042)	5.26×10^7	2.21×10^5
3NPMAF	toluene	480	17 (0.9996), 5354 (0.0004)	5.88×10^7	2.35×10^4
	CH_2Cl_2	568	28 (0.9824), 2083 (0.0176)	3.57×10^7	6.29×10^5
	sublimed powder	508	22 (0.9754), 1338 (0.0246)	4.43×10^7	1.12×10^6
	Co-doped DPEPO film	486	15 (0.9977), 1707 (0.0023)	6.65×10^7	1.53×10^5
4NPMAF	toluene	495	19 (0.9981), 13073 (0.0019)	5.25×10^7	1.00×10^5
	CH_2Cl_2	596	23 (0.9870), 868 (0.0130)	4.29×10^7	5.65×10^5
	sublimed powder	509	12 (0.9820), 570 (0.0180)	8.18×10^7	1.50×10^6
	Co-doped DCDPA film	488	20 (0.9946), 1668 (0.0054)	4.97×10^7	2.70×10^5

[a]Notes that the k_{isc} and k_{risc} are calculated from the kinetic factor of τ_1 and τ_2 in the transient PL decay and the equation are shown below. The subscripts p and d indicates prompt and delay transient signals, respectively. Furthermore, the transient photoluminescence figures were fitted and analyzed by the following equation, assuming the pre-equilibrium between S_1 and T_1 states:

$$I(t) = A_1 \exp\left(-t/\tau_1\right) + A_2 exp(-t/\tau_2) \quad (1)$$

$$k_p = (\tau_1)^{-1}, \quad k_d = (\tau_2)^{-1} \quad (2)$$

$$K_{eq} = \frac{k_{isc}}{k_{risc}} = \frac{A_1}{A_2} \quad (3)$$

$$k_{isc} + k_{risc} = (\tau_1)^{-1} \quad (4)$$

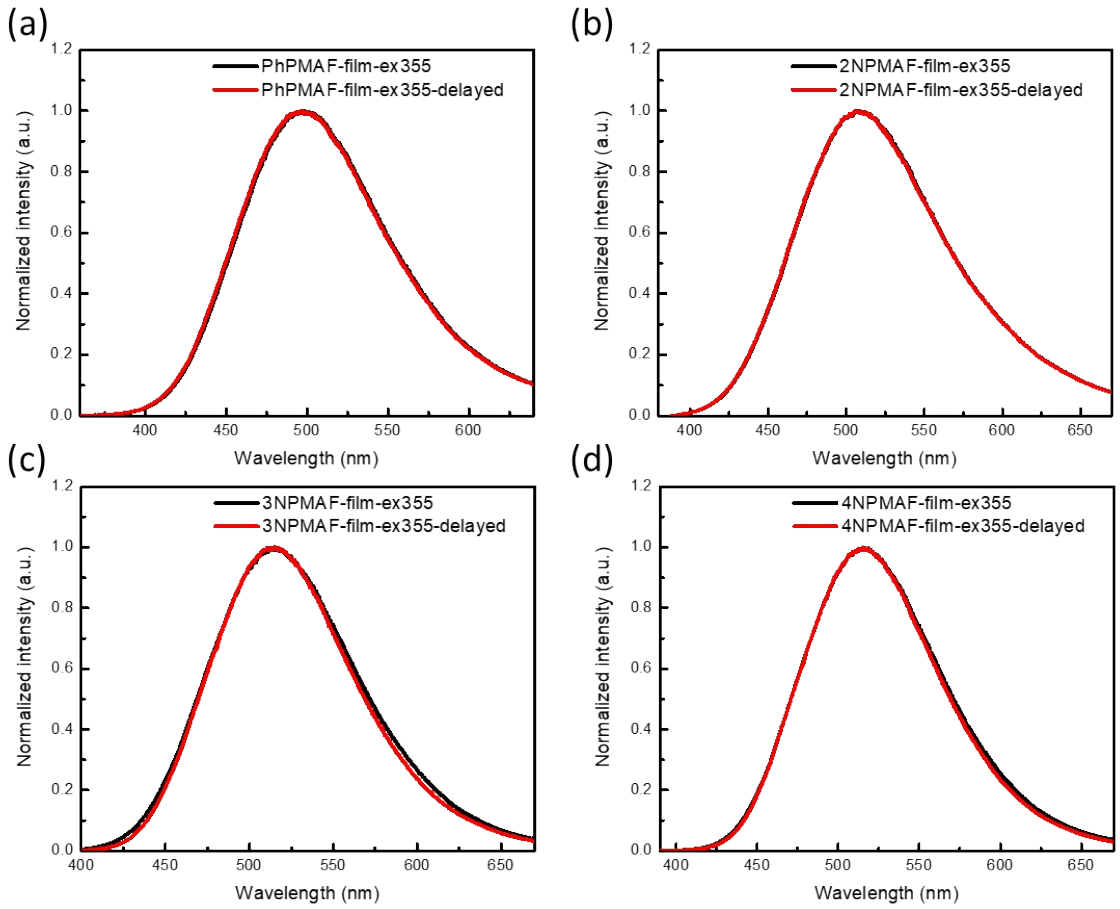

Figure S5. The time resolved PL spectra of the 22 wt.% co-doped films (a) **PhPMAF**, (b) **2NPMAF**, (c) **3NPMAF** and (d) **4NPMAF**. Prompt (black line: delay = 0 ns, gate width = 100 ns) and delayed (red line: delay = 10 μs, gate width = 10 μs) components of PL spectra.

Table S3. Calculated transition wavelength (λ), oscillator strength (*f*) and orbital transition analyses of **PhPMAF**, **2NPMAF**, **3NPMAF** and **4NPMAF**.

complex	State	λ_{cal}	*f*	assignments
PhPMAF	$S_0 \rightarrow S_1$	323.09	0.0000	HOMO→LUMO (72.98%)
				HOMO→LUMO+1 (7.14%)
				HOMO→LUMO+3 (10.20%)
				HOMO→LUMO+4 (2.62%)
	$S_1 \rightarrow S_0$	374.40	0.0015	LUMO→HOMO-4 (91.59%)
2NPMAF	$S_0 \rightarrow S_1$	324.5	0.0000	HOMO→LUMO (56.91%)
				HOMO→LUMO+1 (20.35%)
				HOMO→LUMO+3 (11.36%)
				HOMO→LUMO+4 (2.48%)
	$S_1 \rightarrow S_0$	388.38	0.0013	LUMO→HOMO-3 (91.20%)
3NPMAF	$S_0 \rightarrow S_1$	334.26	0.0001	HOMO→LUMO (67.43%)
				HOMO→LUMO+1 (11.49%)
				HOMO→LUMO+3 (10.69%)
	$S_1 \rightarrow S_0$	389.80	0.0013	LUMO→HOMO (86.72%)
				LUMO+2→HOMO (2.22%)
				LUMO+3→HOMO (3.30%)
4NPMAF	$S_0 \rightarrow S_1$	338.08	0.0000	HOMO→LUMO (59.91%)
				HOMO→LUMO+1 (18.41%)
				HOMO→LUMO+2 (14.29%)
	$S_1 \rightarrow S_0$	381.36	0.0015	LUMO→HOMO-7 (13.19%)
				LUMO→HOMO-6 (15.11%)
				LUMO→HOMO-5 (61.37%)
				LUMO→HOMO-4 (2.15%)

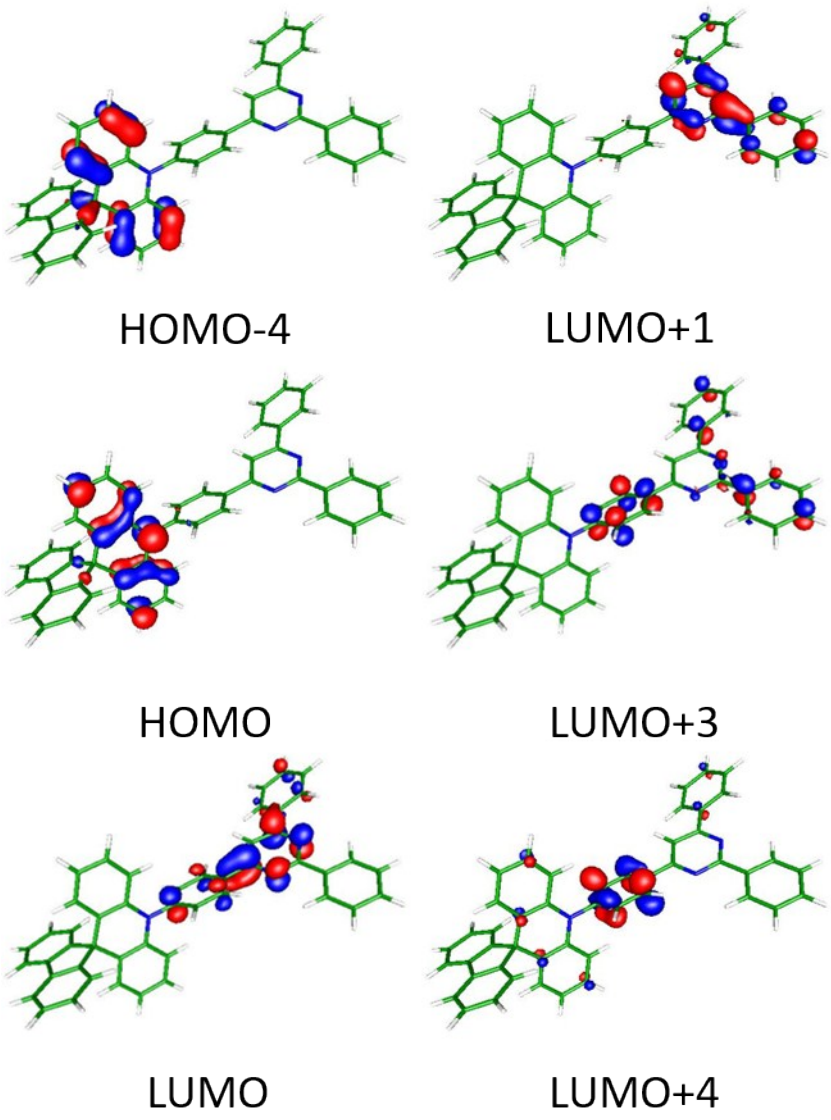

Figure S6. Calculated frontier orbitals of HOMO and LUMO for **PhPMAF** molecule.

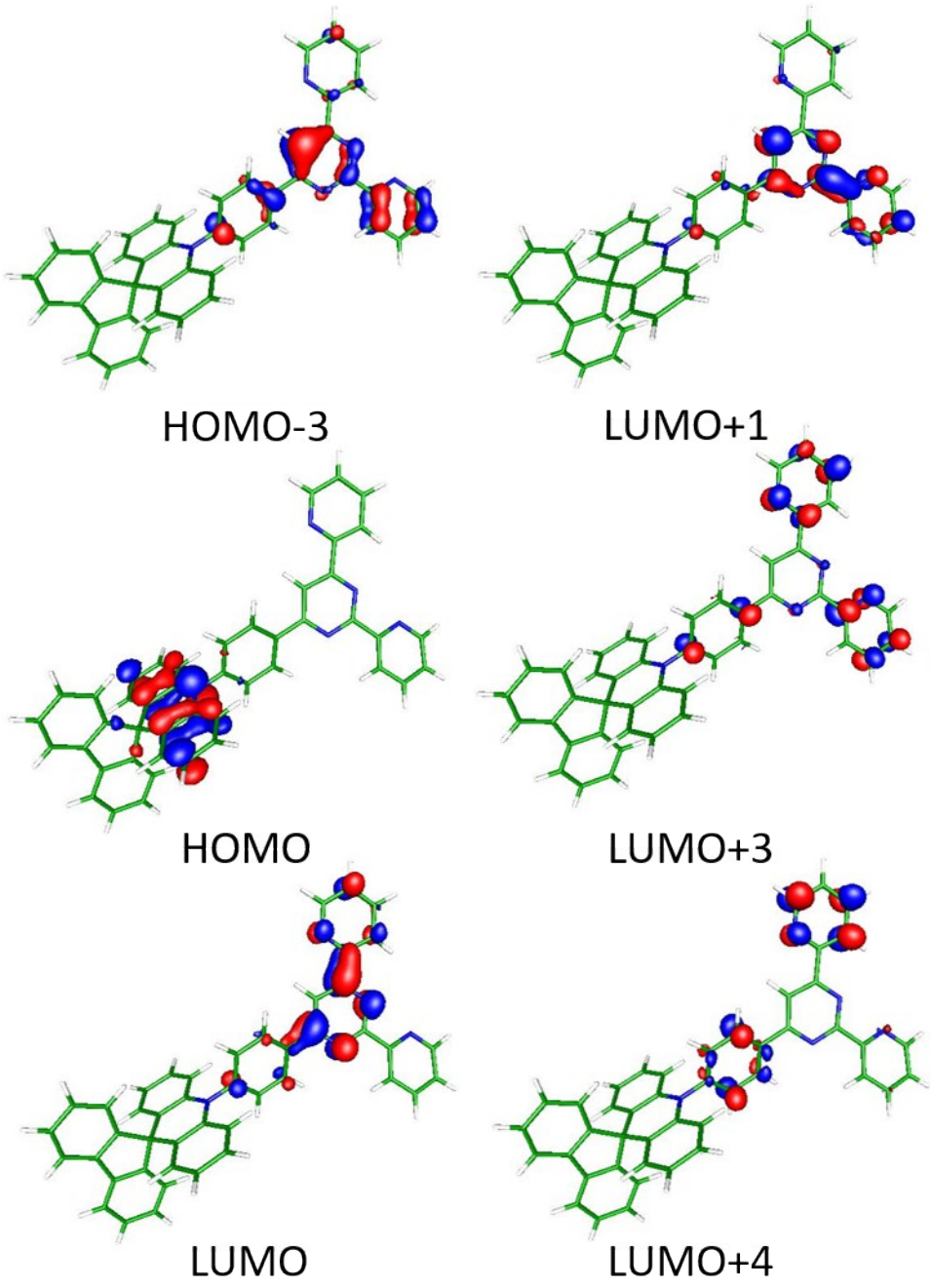

Figure S7. Calculated frontier orbitals of HOMO and LUMO for **2NPMAF** molecule.

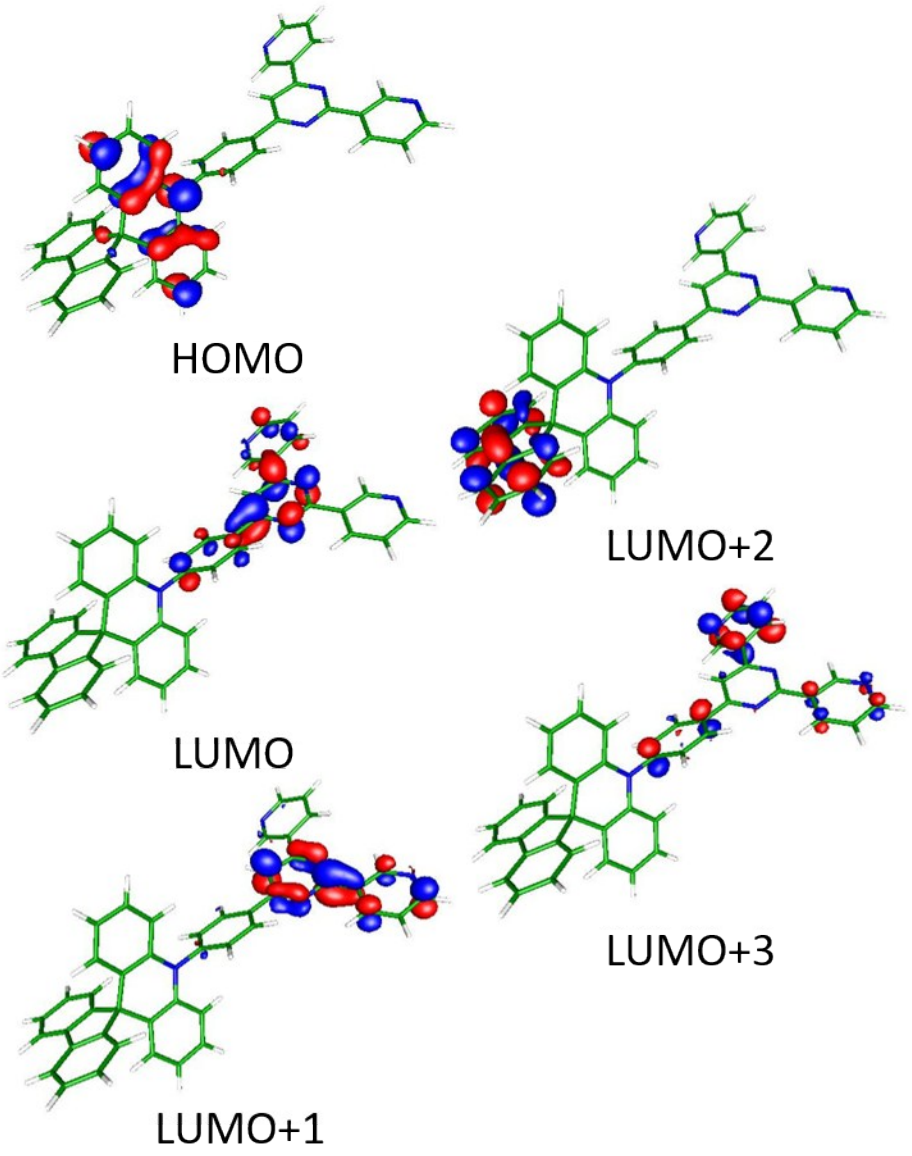

Figure S8. Calculated frontier orbitals of HOMO and LUMO for **3NPMAF** molecule.

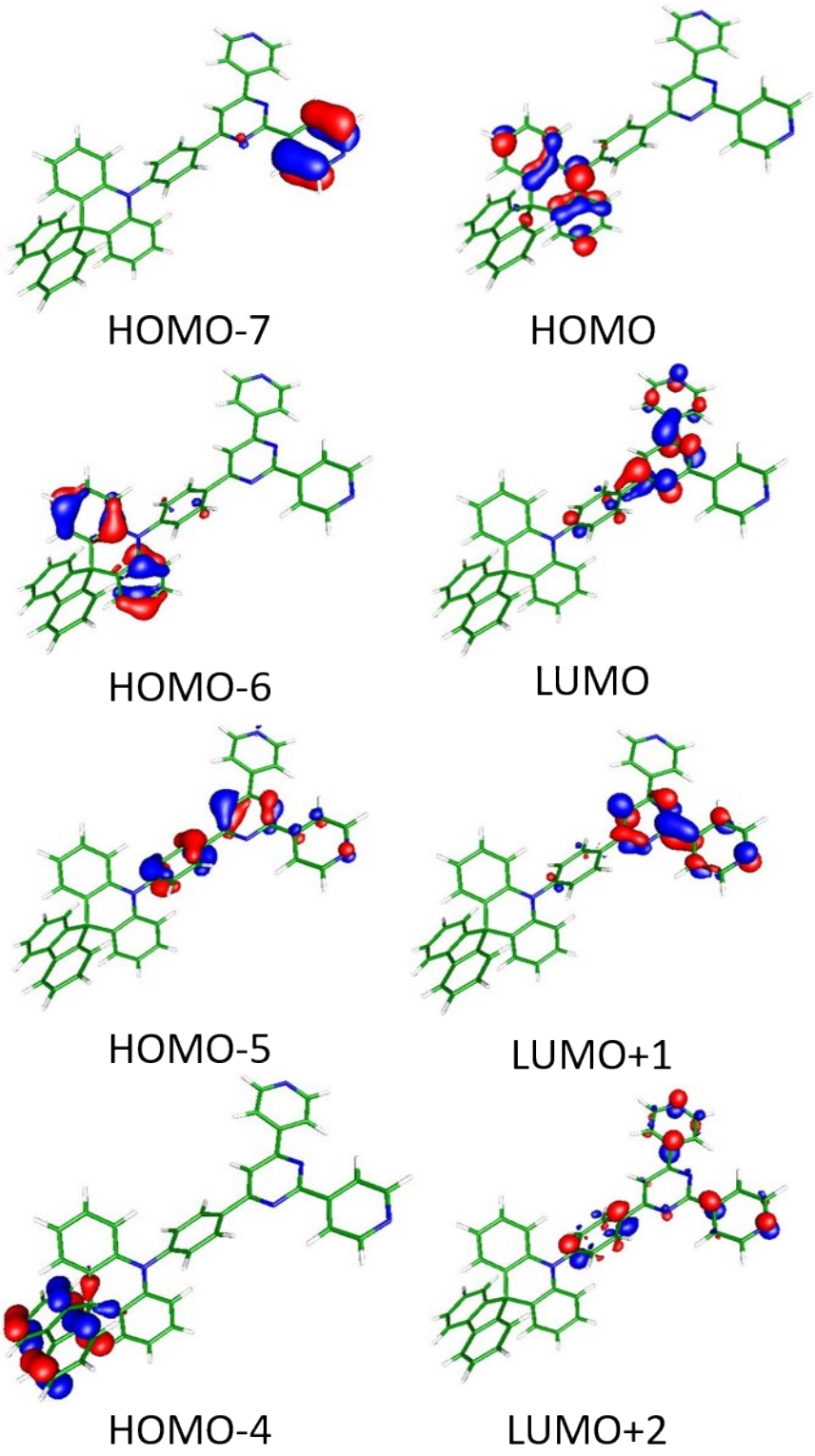

Figure S9. Calculated frontier orbitals of HOMO and LUMO for **4NPMAF** molecule.

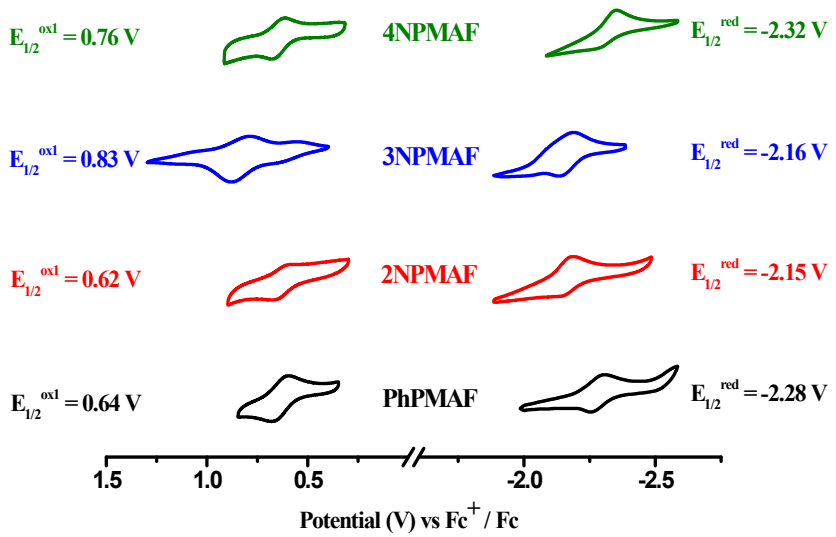

Figure S10. Cyclic voltammograms of **PhPMAF**, **2NPMAF**, **3NPMAF** and **4NPMAF**. The oxidation and reduction experiments were conducted in CH_2Cl_2 and THF solution, respectively. The glassy carbon and gold were selected as the working electrode for oxidation and reduction processes, respectively.

Table S4. Electrochemical properties and calculated bandgaps of the TADF molecules.

SAMPLE CODE	$E_{1/2}^{ox}$ (V)[a]	$E_{1/2}^{red}$ (V)[a]	HOMO (eV) CV[b]	LUMO (eV) CV[b]
PhPMAF	0.64	–2.28	– 5.44	– 2.52
2NPMAF	0.62	– 2.15	– 5.42	– 2.65
3NPMAF	0.83	–2.16	– 5.63	– 2.64
4NPMAF	0.76	– 2.32	– 5.56	– 2.48

[a] $E_{1/2}^{ox}$ and E_{pc}^{re} are the anodic and cathodic peak potentials referenced to the Fc^+/Fc couple. [b] HOMO = $|-4.8 - E_{1/2}^{ox}|$, LUMO = $|-4.8 - E_{pc}^{re}|$.

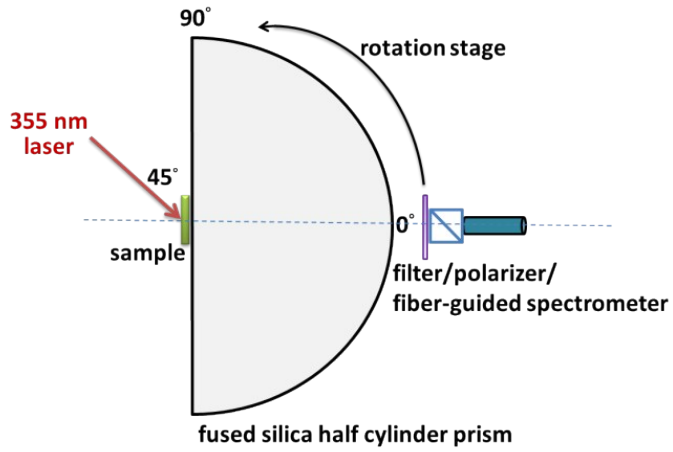

Figure S11. Layout of the experimental setup used for the angle-dependent PL measurement. Note that, in order to analyze the orientation of the transition dipole moment of the emitters, we measured the angular dependence of the *p*-polarised fluorescence intensity. The setup used was as previously described.[4] The experimental setup is composed of a motorized rotation stage, a fused silica-based half cylindrical lens with a sample holder, a longpass filter to stop the excitation beam, a polarizer to select the *p*-polarization of the emitted light and a fiber-guided spectrometer (Ocean Optics USB4000) to collect the PL spectra. A continuous-wave Nd:YAG laser (355 nm, 10 kHz) was used as the excitation source which is fixed behind of sample holder at an incident angle of 45°. The organic layer is evaporated on top of a quartz substrate as a measured sample. The peak intensity of *p*-polarized PL spectra was detected from 0° to 90° in steps of 2° with a fiber-polarizer-spectrometer. The data were analyzed using SETFOS 4.5 (Fluxim AG, Switzerland) to fit the ratio of horizontal dipoles (Θ).

References

[1] M. Numata, T. Yasuda, C. Adachi, *Chem. Commun.* **2015**, *51*, 9443-9446.
[2] T. Sawada, H. Hisada, M. Fujita, *J. Am. Chem. Soc.* **2014**, *136*, 4449-4451.
[3] P. Ganesan, R. Ranganathan, Y. Chi, X.-K. Liu, C.-S. Lee, S.-H. Liu, G.-H. Lee, T.-C. Lin, Y.-T. Chen, P.-T. Chou, *Chem. Eur. J.* **2017**, *23*, 2858-2866.
[4] a) K. S. Yook, S. O. Jeon, C. W. Joo, J. Y. Lee, *Appl. Phys. Lett.* **2008**, *93*, 073302; b) S.-Y. Kim, W.-I. Jeong, C. Mayr, Y.-S. Park, K.-H. Kim, J.-H. Lee, C.-K. Moon, W. Brütting, J.-J. Kim, *Adv. Funct. Mater.* **2013**, *23*, 3896-3900; c) A. Senes, S. C. J. Meskers, W. M. Dijkstra, J. J. van Franeker, S. Altazin, J. S. Wilson, R. A. J. Janssen, *J. Mater. Chem. C* **2016**, *4*, 6302-6308.